Inverse and Direct Energy Cascades in Three-Dimensional Magnetohydrodynamic Turbulence at Low Magnetic Reynolds Number

Nathaniel T. Baker
Coventry University, Applied Mathematics Research Centre, Coventry CV15FB, United Kingdom, LNCMI-EMFL-CNRS, UGA, INSA, UPS 25 Avenue des Martyrs, 38000 Grenoble, France, and Grenoble-INP/CNRS/Université Grenoble-Alpes, SIMaP EPM, F-38000 Grenoble, France

Alban Pothérat
Coventry University, Applied Mathematics Research Centre, Coventry CV15FB, United Kingdom

Laurent Davoust
Grenoble-INP/CNRS/Université Grenoble-Alpes, SIMaP EPM, F-38000 Grenoble, France

François Debray
LNCMI-EMFL-CNRS, UGA, INSA, UPS 25 Avenue des Martyrs, 38000 Grenoble, France

(Received 14 August 2017; published 1 June 2018)

This experimental study analyzes the relationship between the dimensionality of turbulence and the upscale or downscale nature of its energy transfers. We do so by forcing low-Rm magnetohydrodynamic turbulence in a confined channel, while precisely controlling its dimensionality by means of an externally applied magnetic field. We first identify a specific length scale $\hat{l}_{\perp}^{c}$ that separates smaller 3D structures from larger quasi-2D ones. We then show that an inverse energy cascade of horizontal kinetic energy along horizontal scales is always observable at large scales, and that it extends well into the region of 3D structures. At the same time, a direct energy cascade confined to the smallest and strongly 3D scales is observed. These dynamics therefore appear not to be simply determined by the dimensionality of individual scales, nor by the forcing scale, unlike in other studies. In fact, our findings suggest that the relationship between kinematics and dynamics is not universal and may strongly depend on the forcing and dissipating mechanisms at play.

DOI: 10.1103/PhysRevLett.120.224502

Turbulence displays radically opposite dynamics, whether it is three dimensional (3D) or two dimensional (2D). In the former, kinetic energy follows a direct energy cascade from the forcing scale down to the smallest scales [1], while the latter features an inverse energy cascade from the forcing scale up to large structures of the size of the system [2]. It is, however, still unclear how these seemingly irreconcilable dynamics relate to each other, whenever 2D and 3D turbulent structures coexist. This question is all the more crucial when dealing with real-life wall-bounded flows, as speaking of two dimensionality only makes sense with respect to the presence of boundaries, such as no-slip walls. Yet, solid boundaries necessarily introduce three dimensionality both in boundary layers and in the bulk [3,4]. As a result, real flows (such as oceans or atmospheres) can only be quasi-2D rather than strictly 2D, and often combine 2D and 3D turbulent structures [5]. The key question that determines both transport and dissipative properties of such flows is then how much, and which kind of three dimensionality is required for the inverse cascade to become direct. In other words: How do the energy transfers relate to the topological dimensionality of turbulence?

It is unclear whether this question has a universal answer. For instance, compressing one dimension can yield a hybrid configuration, in which the energy flux splits into a direct cascade at small scales and an inverse cascade at large scales [6], while forcing a 3D and three-component flow in a thick fluid layer can still produce a large coherent vortex, indicative of an upscale energy flux [7]. Furthermore, within the respective contexts of rotating [8], and stratified rotating quasi-2D turbulence [9], horizontal kinetic energy flows preferentially upscale, while vertical kinetic energy flows downscale. Finally, a subset of the nonlinear interactions of any 3D flow is always capable of transferring kinetic energy upscale [10].

This matter is investigated within the context of statistically steady liquid metal low-Rm magnetohydrodynamic (MHD) turbulence in a homogeneous magnetic field [11–13]. A significant advantage of this approach is that the level of three dimensionality of MHD turbulence can be controlled simply by adjusting the external magnetic field $\mathbf{B}_0$ [14–17]. In particular, Ref. [18] theorized that a critical length scale separates (larger) quasi-2D from (smaller) 3D turbulent structures, by interpreting the effect of the

solenoidal component of the Lorentz force as a "pseudo-diffusion" of momentum in the direction of the magnetic field. The time $\tau_{2D}(l_\perp)$ required to diffuse the momentum of a turbulent structure of size $l_\perp$ over the distance l_z along $\mathbf{B}_0$ is given by $\tau_{2D} = (\rho/\sigma B_0^2)(l_z/l_\perp)^2$, where σ and ρ are the fluid's electric conductivity and density, respectively. In the inertial range, the other competing process is inertia, whose main effect is to redistribute kinetic energy across turbulent structures, by means of energy transfers. It takes place over the eddy turnover time $\tau_u(l_\perp) = l_\perp/u(l_\perp)$, where $u(l_\perp)$ is the velocity of the structure at hand. The scaling law for the range of action of the Lorentz force follows from the balance between both effects [18]:

$$l_z(l_\perp) = l_\perp\sqrt{N(l_\perp)}, \tag{1}$$

where $N(l_\perp, u(l_\perp)) = \sigma B_0^2 l_\perp/\rho u(l_\perp)$ is a scale-dependent interaction parameter. The dimensionality of a structure is then determined with respect to no-slip walls perpendicular to the magnetic field and distant by h, through the ratio $l_z(l_\perp)/h$ [19,20]. In particular, $l_z(l_\perp)/h \leq 1$ implies that velocity gradients exist in the bulk, in other words, that the structure of size $l_\perp$ is 3D. Conversely, $l_z(l_\perp)/h \gg 1$ implies that the Lorentz force diffuses the momentum of the structure of size $l_\perp$ over a distance much greater than h. This process is, however, blocked by the no-slip walls. The structure of size $l_\perp$ is thus quasi-2D. The critical length scale $l_\perp^c$ separating quasi-2D and 3D structures, for which $l_z(l_\perp^c)/h = 1$, eventually reads [18]

$$\frac{l_\perp^c}{h} \sim \left(\frac{\sigma B_0^2 h}{\rho u(l_\perp^c)}\right)^{-1/3} = N(h, u(l_\perp^c))^{-1/3}. \tag{2}$$

Increasing the applied magnetic field thus offers a convenient way of broadening the spectrum of quasi-2D scales.

The problem at hand was tackled experimentally using the Flowcube [19,21–23], an experimental platform designed to drive turbulence electrically in a $100 \times 100 \times 150$ mm parallelepipedic vessel, filled with a GaInSn eutectic alloy ($\rho = 6400$ kg/m^3, $\sigma = 3.4 \times 10^6$ S/m, kinematic viscosity $\nu = 4.0 \times 10^{-7}$ m^2/s). Turbulent motions were induced by forcing a dc electric current I_0 through a square periodic array of electrodes spaced either by $l_i = 5$ or 15 mm located along the bottom wall [21], while simultaneously applying a vertical and static magnetic field $B_0\mathbf{e}_z$, of up to 10 T (cf. Fig. 1). Two complementary measurement methods were used to diagnose the resulting flow. First, a fine Cartesian mesh of probes mounted flush to the top and bottom walls along strips aligned with the $\mathbf{e}_x$ direction gave access to the electric potential distribution at these walls. The spatial resolution of this method, as given by the spacing between adjacent probes was 2.5 mm. The signal was time sampled at 250 Hz/24-bits over 18 mn-long continuous runs. In the limit of high Hartmann numbers ($\mathrm{Ha} = B_0 h\sqrt{\sigma/\rho\nu}$) and high interaction parameter, the electric potential along the horizontal walls is a precise

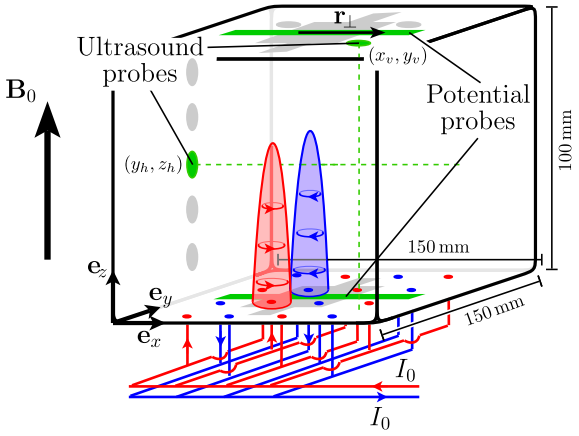

FIG. 1. Sketch of the Flowcube.

estimate for the stream-function right outside the Hartmann boundary layer developing along them [24]. It thus provides both velocity components in the same planes. Second, two ultrasound transducers were used to respectively measure the $u_x(x, y_h, z_h, t)$ and $u_z(x_v, y_v, z, t)$ velocity profiles through the bulk, at the fixed positions (y_h, z_h) and (x_v, y_v), respectively. The transducers offered a spatial resolution of $\sim$1 mm, and a 5 Hz sampling rate. The dimensionality of the flow was controlled through the single parameter $l_z(l_i)/h$, where $l_z(l_i)$ is the diffusion length associated to turbulent structures of size l_i and the rms of the turbulent fluctuations measured along the bottom wall u_{bot} [21]. The Reynolds number $\mathrm{Re} = u_{\mathrm{bot}}h/\nu$ ranged between 17 000 and 71 000 throughout, which guaranteed that the turbulence was fully developed. The Hartmann number and Magnetic Reynolds number $\mathrm{Rm} = \mu_0\sigma u_{\mathrm{bot}}h$ (μ_0 referring to vacuum permitivity), ranged between 911 and 36 400, and 0.029 and 0.12, respectively. Selected regimes achievable by the Flowcube are given in Table I. Except for Fig. 4, the statistics presented hereafter stem from data acquired by potential measurements. The average operator must be understood as an ensemble average obtained by averaging over time and space. Statistics were computed using $\sim 10^7$ independent samples, which yielded a convergence level better than 1% for the third order moments [21].

Following Ref. [25], we describe the structure of turbulence through the velocity increment $\delta\mathbf{u} = \mathbf{u}(\mathbf{x}+\mathbf{r}) - \mathbf{u}(\mathbf{x})$, computed from turbulent fluctuations. Because of the very low influence from the lateral walls [21], the turbulence in Flowcube is considered homogeneous in the horizontal plane and axisymmetric. Hence, $\mathbf{r}$ and $\delta\mathbf{u}$ are, respectively, decomposed as $\mathbf{r} = r_\perp\mathbf{e}_r + r_\parallel\mathbf{e}_z$ and $\delta\mathbf{u} = \delta\mathbf{u}_\perp + \delta\mathbf{u}_\parallel$, with $\delta\mathbf{u}_\parallel = (\delta\mathbf{u}\cdot\mathbf{e}_z)\mathbf{e}_z$ and $\delta\mathbf{u}_\perp = \delta\mathbf{u} - \delta\mathbf{u}_\parallel$. We shall focus on $\delta\mathbf{u}_\perp(r_\perp\mathbf{e}_x)$ computed along both the top and bottom plates.

Let us start by analyzing the kinematics of the turbulence and attempt to discriminate 3D from quasi-2D structures. To do so, we adopt the signature function V as a scale-space alternative to the Fourier-space 3D energy spectrum [26], which is expressed in 2D as [27]

TABLE I. Range of nondimensional parameters for an injected current per electrode of 6A. Data are given for both electrode separations l_i, and a selected range of magnetic fields (cf. Ref. [21] for more details).

$l_i = 5$ mm					
B_0[T]	1	3	5	7	10
u_{bot}[m/s]	0.180	0.230	0.240	0.250	0.270
Ha	3644	10 930	18 220	25 510	36 440
Re	44 000	58 000	60 000	64 000	67 000
$l_z(l_i)/h$	0.23	0.59	0.97	1.3	1.7
$l_i = 15$ mm					
B_0[T]	1	3	5	7	10
u_{bot}[m/s]	0.130	0.180	0.200	0.230	0.250
Ha	3644	10 930	18 220	25 510	36 440
Re	32 000	45 000	50 000	57 000	62 000
$l_z(l_i)/h$	1.3	3.4	5.3	6.9	9.4

$$V_\perp(r_\perp) = -\frac{r_\perp^2}{4}\frac{\partial}{\partial r_\perp}\frac{1}{r_\perp}\frac{\partial\langle\delta u_l^2\rangle}{\partial r_\perp}. \tag{3}$$

Here, $\delta u_l = [\mathbf{u}(\mathbf{x} + r_x\mathbf{e}_x) - \mathbf{u}(\mathbf{x})]\cdot\mathbf{e}_x$ is the longitudinal velocity increment measured in the horizontal plane. In axisymmetric turbulence, quasi-2D structures are invariant with respect to z outside the boundary layers. Their signature function must therefore be the same whether measured along the top or bottom walls. Conversely, any departure from a top-bottom mirror symmetry is an indication of a 3D structure. Figure 2 shows the scalewise distribution of $V_\perp(r_\perp)$ across horizontal structures, along the top and bottom walls (referred to as $V_\perp^{\mathrm{top}}$ and $V_\perp^{\mathrm{bot}}$ respectively). As $l_z(l_i)/h$ increases beyond one, $V_\perp^{\mathrm{top}}$ tends to match $V_\perp^{\mathrm{bot}}$, both in shape and amplitude. Based on this observation, a lower bound for the smallest quasi-2D scale is computed from the location of $V_\perp^{\mathrm{top}}(r_\perp)$'s maximum $\hat{l}_\perp^c$. Interestingly, the superposition of top and bottom energy distributions starts at large scales and works its way through smaller and smaller scales as $l_z(l_i)/h$ increases. This behavior is in full agreement with Eq. (1), which states that it takes a higher field [i.e., a higher $l_z(l_i)/h$] to make smaller structures quasi-2D. Furthermore, the critical length scale $\hat{l}_\perp^c$ strikingly coincides with the scale at which $V_\perp^{\mathrm{bot}}$ and $V_\perp^{\mathrm{top}}$ depart from each other, thus confirming its physical relevance.

Figure 3 reports the variations of $\hat{l}_\perp^c/l_i$ for all operating conditions explored against the "true" interaction parameter $N_t = N(h, u_\perp^c)\times(l_i/h)^2 = [l_z(l_i)/h]^2(h/l_i)$, which measures the ratio of diffusion by the Lorentz force to inertia at the forcing scale [28]. Here, $u_\perp^c = [2V_\perp^{\mathrm{top}}(\hat{l}_\perp^c)\hat{l}_\perp^c]^{1/2}$ is an estimate for the velocity at scale $\hat{l}_\perp^c$. All measurements collapse onto a single curve, of which two parts can be singled out. For $N_t \lesssim 10^2$, $\hat{l}_\perp^c/l_i \propto {N_t}^{-1/3}$, which provides

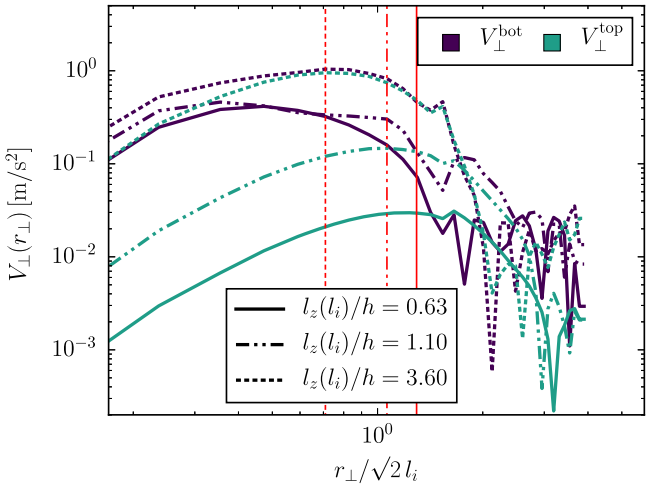

FIG. 2. Scalewise perpendicular energy density along horizontal scales. Normalization by $\sqrt{2}$ is introduced so that the abscissae of Figs. 2 and 5 coincide with each other (cf. properties of $V_\perp$ in Ref. [27]). The vertical red lines locate $\hat{l}_\perp^c/l_i$ for each $l_z(l_i)/h$, with quasi-2D scales lying to their right.

an experimental confirmation of Eq. (2). For $N_t \gtrsim 10^2$, $\hat{l}_c/l_i$ saturates towards a constant value of 0.62, indicating that scales below this limit size cannot be quasi-2D no matter how high N_t might be. This limit likely results from the absence of a mechanism to transfer energy to 2D scales smaller than the energy injection scale, a phenomenon which is not accounted for in Eq. (2).

Having identified quasi-2D and 3D regions of the scale space, we now seek regions where energy is transferred upscale and downscale. We first recall that the equation governing energy transfers in statistically steady MHD

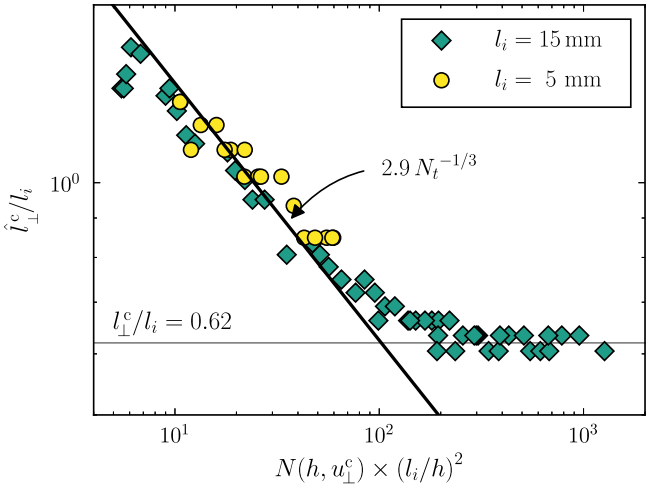

FIG. 3. 3D to quasi-2D critical length scale $\hat{l}_\perp^c$, as a function of the "true" interaction parameter $N_t = N(h, u_\perp^c)\times(l_i/h)^2$. The ${N_t}^{-1/3}$ region proves that the threshold between 3D and quasi-2D structures is indeed solely controlled by a balance between the solenoidal component of the Lorentz force and inertia.

turbulence is the Kàrmàn-Howarth equation, which reads, in the inhomogeneous and anisotropic case [29]

$$\Pi(\mathbf{r}) = \mathcal{P}(\mathbf{r}) + \mathcal{T}(\mathbf{r}) - \epsilon_J(\mathbf{r}) - \epsilon_\nu(\mathbf{r}). \quad (4)$$

$\Pi(\mathbf{r}) = \nabla_{\mathbf{r}} \cdot \langle |\delta\mathbf{u}|^2 \delta\mathbf{u} \rangle$ quantifies the flux of turbulent kinetic energy in scale space, $\mathcal{P}(\mathbf{r})$ is the rate of production of turbulent kinetic energy, $\mathcal{T}(\mathbf{r})$ is the flux of turbulent kinetic energy in physical space (due to spatial inhomogeneities), ϵ_J is the Joule dissipation (occurring in the bulk and the Hartmann layers [12]), while ϵ_ν represents viscous dissipation. In low-Rm MHD, the energy transfers remain confined to the usual nonlinear hydrodynamic term $\Pi(\mathbf{r})$, which represents a local cumulative flux of kinetic energy exchanged between scales of size $r = \|\mathbf{r}\|$ and less, with those of size r and greater [8]. More specifically, $\Pi(r) > 0$ [respectively, $\Pi(r) < 0$] implies that, on average, energy flows towards scales larger (respectively, smaller) than r, i.e., following an inverse (respectively, direct) energy cascade. Invoking axisymmetry, $\Pi(\mathbf{r})$ becomes a function of $r_\perp$ and $r_\parallel$ only, and splits into the four contributions [8,9]

$$\Pi_\alpha^\beta = \nabla_\alpha \cdot \langle |\delta\mathbf{u}_\beta|^2 \delta\mathbf{u}_\alpha \rangle, \quad (5)$$

where α and β independently represent $\perp$ or $\parallel$, $\nabla_\perp \cdot = (1/r_\perp)\partial_{r_\perp}(r_\perp \cdot)$, and $\nabla_\parallel \cdot = (\partial_{r_\parallel} \cdot) \cdot \mathbf{e}_z$. None of $\Pi_\perp^\parallel$, $\Pi_\parallel^\perp$, or $\Pi_\parallel^\parallel$ can be precisely obtained from our measurements. Estimates for all contributions may nevertheless be computed as $\hat{\Pi}_\alpha^\beta = \langle \mathbf{u}_\beta^2 \rangle \sqrt{\langle \mathbf{u}_\alpha^2 \rangle}/l_\alpha$, with $l_\perp = l_i$ and $l_\parallel = l_z(l_i)$. Figure 4 shows all $\hat{\Pi}_\alpha^\beta$ against $l_z(l_i)/h$. The normalization involves $l_z(l_i)$ and $E_0 = [\langle \mathbf{u}_\perp^2 \rangle + \langle \mathbf{u}_\parallel^2 \rangle]/2$ to account for the different energy levels. The only contribution to the energy transfers that strengthens, as the flow becomes quasi-2D is $\hat{\Pi}_\perp^\perp$. This reflects that in quasi-2D channel flows, (i) the vertical velocity component becomes very small compared to the horizontal one [21,30], and (ii) velocity gradients along the magnetic field vanish. Consequently, any contribution to Π involving $\delta\mathbf{u}_\parallel$ and/or $\partial_{r_\parallel}$ must dwindle with $l_z(l_i)/h$. In the quasi-2D limit [i.e., $l_z(l_i)/h \to \infty$], $\Pi_\perp^\perp$ coincides with Π. In any case, since $\Pi_\perp^\perp$ remains greater than the sum of all other contributions, whether the flow is 3D or not, $\Pi_\perp^\perp$ is representative of the total energy transfer Π.

In 3D MHD turbulence, Joule dissipation induces energy losses at all scales. The inertial range is accordingly reduced, and small-scale viscous dissipation is negligible when $N \gg 1$. Conversely, quasi-2D scales only experience significant dissipation through friction in the Hartmann layers if their turnover time exceeds the Hartmann friction time $\tau_H = h^2/\nu\mathrm{Ha}$. In other words, energy is not conservatively transferred across the inertial range of MHD turbulence whether up- or downscale. Hence, the energy cascade does not necessarily incur a plateau region of constant energy flux. The sign of $\Pi_\perp$ is, however, enough to determine the direction of the transfer, as in Refs. [3,8,9,31]. Note that none of our experiments displayed condensation into large turbulent structures, unlike other comparable studies [7,32,33]. This is due to a natural energy sink at large quasi-2D scales in the form of Hartmann friction, which always acted at an intermediate scale between the size of the forced region and that of the domain. This specific feature of the Flowcube ultimately enabled us to sustain statistically steady turbulence over long times.

Figure 5 displays the horizontal transfer of horizontal kinetic energy between horizontal scales $\Pi_\perp^\perp(r_\perp)$, computed along the top and bottom Hartmann walls (referred to as $\Pi_\perp^{\mathrm{top}}$ and $\Pi_\perp^{\mathrm{bot}}$, respectively). The bulk of the transfers

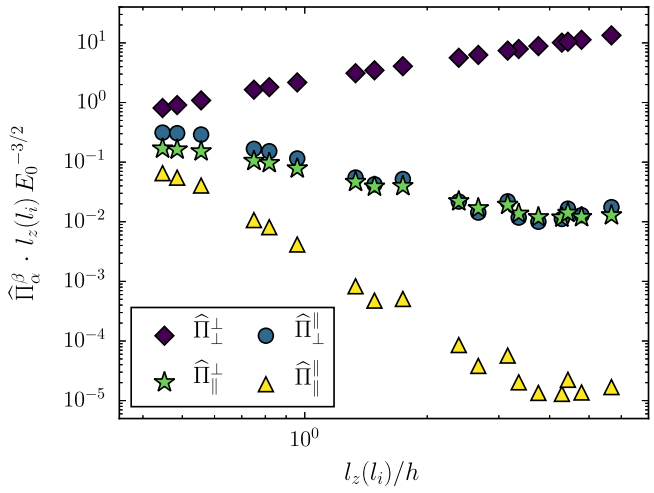

FIG. 4. Global estimates for the different contributions to Π, computed from ultrasound measurements. Regardless of the dimensionality of the flow, the main contribution to the cascade is $\Pi_\perp^\perp$, which can accurately be measured using potential probes.

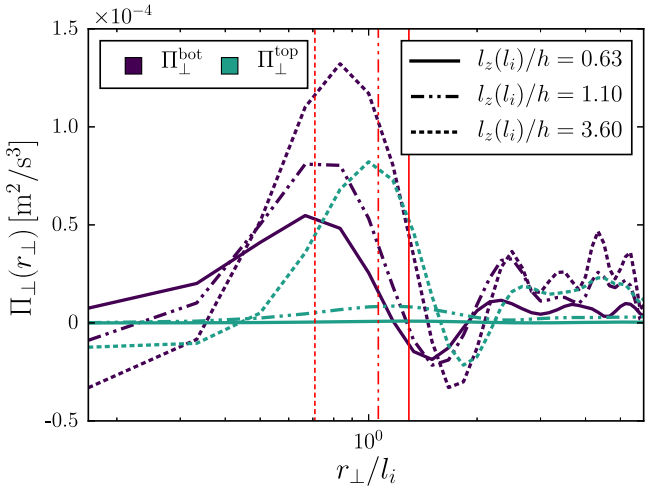

FIG. 5. Horizontal transfers of horizontal turbulent kinetic energy along the top and bottom walls, showing an inverse cascade ($\Pi_\perp > 0$) at large scales. Counterintuitively, two dimensionalization *promotes* a direct cascade ($\Pi_\perp < 0$) at smaller scales. Red lines locate $\hat{l}_\perp^c/l_i$.

occurs in the range $r_\perp/l_i \geq 0.4$, for which $\Pi_\perp^{\mathrm{bot}}(r_\perp)$ and $\Pi_\perp^{\mathrm{top}}(r_\perp)$ are overall positive, thus indicating an upscale energy flux. The upper end of this region is dominated by oscillations, whose wavelength is close to l_i. These oscillations, therefore, likely result from the spatial inhomogeneities introduced by the forcing pattern, and/or by the nonrandom formation and breakup of forced vortex pairs [23,34,35]. The floor of these oscillations lies, however, well above noise level, which confirms, together with the continuous nature of the signature function, that random energy transfers add-up to an upscale flux at larger scales. Indeed, nonrandom energy transfers would translate into energy being exclusively localized at selected wavelengths only. This picture is consistent with direct numerical simulations (DNS) in periodic domains [36] showing that the energy cascade in MHD turbulence is local and inverse at large scales. Surprisingly, the inverse cascade extends well below $\hat{l}_\perp^c$, implying that 3D scales can also sustain an inverse cascade. What is more, two dimensionality simultaneously promotes a direct cascade at the lower end of the spectrum (indicated by a negative value of $\Pi_\perp^+$), at scales lying below the saturation scale observed in Fig. 2. This behavior confirms the presence of irreducible three dimensionality at the smallest scales. While it is not surprising that quasi-2D structures always undergo an inverse cascade, it is remarkable that some 3D scales do, and that the direct cascade affects a wider range of small scales, while two dimensionality is promoted. These observations contrast with DNS of partly 2D and partly 3D turbulence [6,10,37], which feature sharp cascade inversions at the forcing scale only. This crucial difference may be explained by the presence of strong Joule dissipation in our setup [31,36], and/or the "broadband" nature of our forcing.

To conclude, this study shows that energy transfers are not simply governed by the topological dimensionality of turbulence, but may also depend on the mechanisms promoting two dimensionality and/or dissipation. In particular, MHD turbulence provides a remarkable example where an inverse energy cascade extends to topologically 3D scales. The link between turbulence kinematics and dynamics is therefore unlikely to be universal and calls for a new understanding.

A. P. acknowledges support from the Royal Society (Wolfson Research Merit Award Grant No. WM140032, International Exchanges Grant No. 140127), and invited professorships from Grenoble-INP and Université Grenoble-Alpes. The SIMaP laboratory is part of the LabEx Tec 21 (Investissements d'Avenir—Grant No. ANR-11-LABX-0030).

[1] L. Richardson, *Weather Prediction by Numerical Process* (Cambridge University, Cambridge, England, 1922).
[2] R. Kraichnan, Inertial ranges in two-dimensional turbulence, Phys. Fluids **10**, 1417 (1967).
[3] J. Paret, D. Marteau, O. Paireau, and P. Tabeling, Are flows electromagnetically forced in thin stratified layers two dimensional?, Phys. Fluids **9**, 3102 (1997).
[4] R. A. D. Akkermans, L. P. J. Kamp, H. J. H. Clercx, and G. H. F. Van Heijst, Intrinsic three-dimensionality in electromagnetically driven shallow flows, Europhys. Lett. **83**, 24001 (2008).
[5] E. Lindborg, Can the atmospheric kinetic energy spectrum be explained by two-dimensional turbulence?, J. Fluid Mech. **388**, 259 (1999).
[6] A. Celani, S. Musacchio, and D. Vincenzi, Turbulence in More than Two and Less than Three Dimensions, Phys. Rev. Lett. **104**, 184506 (2010).
[7] H. Xia, D. Byrne, G. Falkovich, and M. Shats, Upscale energy transfer in thick turbulent fluid layers, Nat. Phys. **7**, 321 (2011).
[8] A. Campagne, B. Gallet, F. Moisy, and P.-P. Cortet, Direct and inverse energy cascades in a forced rotating turbulence experiment, Phys. Fluids **26**, 125112 (2014).
[9] R. Marino, P. D. Mininni, D. L. Rosenberg, and A. Pouquet, Large-scale anisotropy in stably stratified rotating flows, Phys. Rev. E **90**, 023018 (2014).
[10] G. Sahoo, A. Alexakis, and L. Biferale, Discontinuous Transition from Direct to Inverse Cascade in Three-Dimensional Turbulence, Phys. Rev. Lett. **118**, 164501 (2017).
[11] P. Davidson, *An Introduction to Magnetohydrodynamics* (Cambridge University Press, Cambridge, England, 2001).
[12] B. Knaepen and R. Moreau, Magnetohydrodynamic turbulence at low magnetic Reynolds number, Annu. Rev. Fluid Mech. **40**, 25 (2008).
[13] M. Verma, Anisotropy in quasi-static magnetohydrodynamic turbulence, Rep. Prog. Phys. **80**, 087001 (2017).
[14] H. K. Moffatt, On the suppression of turbulence by a uniform magnetic field, J. Fluid Mech. **28**, 571 (1967).
[15] A. Alemany, R. Moreau, P. Sulem, and U. Frisch, Influence of an external magnetic field on homogeneous MHD turbulence, J. Méc. **18**, 277 (1979).
[16] S. Eckert, G. Gerbeth, W. Witke, and H. Langenbrunner, MHD turbulence measurements in a sodium channel flow exposed to a transverse magnetic field, Int. J. Heat Fluid Flow **22**, 358 (2001).
[17] K. Messadek and R. Moreau, An experimental investigation of MHD quasi-two-dimensional turbulent shear flows, J. Fluid Mech. **456**, 137 (2002).
[18] J. Sommeria and R. Moreau, Why, how and when MHD turbulence becomes two-dimensional, J. Fluid Mech. **118**, 507 (1982).
[19] A. Pothérat and R. Klein, Why, how and when MHD turbulence at low-Rm becomes three-dimensional, J. Fluid Mech. **761**, 168 (2014).
[20] N. T. Baker, A. Pothérat, and L. Davoust, Dimensionality, secondary flows and helicity in low-Rm MHD vortices, J. Fluid Mech. **779**, 325 (2015).
[21] N. T. Baker, A. Pothérat, L. Davoust, F. Debray, and R. Klein, Controlling the dimensionality of low-Rm MHD turbulence experimentally, Exp. Fluids **58**, 79 (2017).
[22] A. Pothérat and R. Klein, Do magnetic fields enhance turbulence at low magnetic Reynolds number?, Phys. Rev. Fluids **2**, 063702 (2017).

[23] R. Klein and A. Pothérat, Appearance of Three-Dimensionality in Wall Bounded MHD Flows, Phys. Rev. Lett. **104**, 034502 (2010).
[24] A. Kljukin and A. Thess, Direct measurement of the streamfunction in a quasi-two-dimensional liquid metal flow, Exp. Fluids **25**, 298 (1998).
[25] C. Lamriben, P.-P. Cortet, and F. Moisy, Direct Measurements of Anisotropic Energy Transfers in a Rotating Turbulence Experiment, Phys. Rev. Lett. **107**, 024503 (2011).
[26] P. A. Davidson and B. R. Pearson, Identifying Turbulent Energy Distributions in Real, Rather than Fourier, Space, Phys. Rev. Lett. **95**, 214501 (2005).
[27] P. Davidson, *Turbulence: An Introduction for Scientists and Engineers* (Oxford University Press, New York, 2015).
[28] B. Sreenivasan and T. Alboussière, Experimental study of a vortex in a magnetic field, J. Fluid Mech. **464**, 287 (2002).
[29] R. Hill, Exact second-order structure-function relationships, J. Fluid Mech. **468**, 317 (2002).
[30] A. Pothérat and K. Kornet, The decay of wall-bounded MHD turbulence at low-Rm, J. Fluid Mech. **783**, 605 (2015).
[31] B. Favier, F. S. Dodeferd, C. Cambon, A. Delache, and W. J. T. Bos, Quasi-static magnetohydrodynamic turbulence at high Reynolds number, J. Fluid Mech. **681**, 434 (2011).
[32] J. Paret and P. Tabeling, Intermittency in the two-dimensional inverse cascade of energy: Experimental observations, Phys. Fluids **10**, 3126 (1998).
[33] J. Sommeria, Experimental study of the two-dimensional inverse energy cascade in a square box, J. Fluid Mech. **170**, 139 (1986).
[34] P. Tabeling, Two-dimensional turbulence: A physicist approach, Phys. Rep. **362**, 1 (2002).
[35] A. Thess, Instabilities in two-dimensional periodic flows part iii: Square eddy lattice, Phys. Fluids A **4**, 1396 (1992).
[36] K. S. Reddy, R. Kumar, and M. K. Verma, Anisotropic energy transfers in quasi-static magnetohydrodynamic turbulence, Phys. Plasmas **21**, 102310 (2014).
[37] K. Seshasayanan, S. J. Benavides, and A. Alexakis, On the edge of an inverse cascade, Phys. Rev. E **90**, 051003 (2014).